

A Dynamical Model for the Orbit of the Andromeda Galaxy M31 and the Origin of the Local Group of Galaxies

Takeyasu SAWA

Department of Physics and Astronomy, Aichi University of Education, Kariya 448-8542
tsawa@aeucc.aichi-edu.ac.jp

and

Mitsuaki FUJIMOTO

Temporary address: U-Lab, Department of Physics and Astrophysics, Nagoya University, Nagoya 464-8602
fujimoto@a.phys.nagoya-u.ac.jp

(Received ⟨reception date⟩; accepted ⟨acceptance date⟩)

Abstract

We propose a new model for the origin and evolution of the Local Group of Galaxies (LGG) which naturally explains the formation of the Magellanic Clouds and their large orbital angular momenta around the Galaxy. The basic idea is that an off-center hydrodynamical collision occurred some 10 Gyr ago between the primordial gas-rich Andromeda galaxy and the similar Galaxy, and compressed the halo gas to form the LGG dwarf galaxies including the Magellanic Clouds. In this model, new-born dwarf galaxies can be expected to locate near the orbital plane of these two massive galaxies. In order to see the reality of this model, we reexamine the two-dimensional sky distribution of the LGG members and the Magellanic Stream, we confirm an earlier and widely-discussed idea that they align along two similar great circles, each with an angular width of $\sim 30^\circ$, and the planes of these circles are approximately normal to the line joining the present position of the sun and the Galactic center. Further we make a three-dimensional distribution map of these objects, and observe it from various directions. A well-defined plane of finite thickness is found, within which most of the member galaxies are confined, supporting the existence of the above circles on the sky. Thus we could determine the orbital elements of M31 relative to the Galaxy through reproducing the well-studied dynamics of the LMC and the SMC around the Galaxy. The expected proper motion of M31 is $(\mu_l, \mu_b) = (38 \mu\text{as yr}^{-1}, -49 \mu\text{as yr}^{-1})$. Probable orbital motions of the other dwarfs are also determined, and the corresponding proper motion for each object is given to compare with observations in near future.

Key words: galaxies: formation — galaxies: kinematics and dynamics — galaxies: Local Group

1. Introduction

In spite of extensive observational/theoretical studies of the Magellanic Clouds, their origins remain unsolved for a long time. Did they initially form as satellite galaxies of the Galaxy, or did they fall into the Galaxy in the course of dynamical evolution of the LGG (Byrd et al. 1994). A more realistic hint to this problem can be presented by studies of the origin of the Magellanic Stream (MS). Tidal models have been successfully introduced to the dynamics of the Galaxy-LMC-SMC system for reproducing the geometrical and dynamical structure of the MS (Murai & Fujimoto 1980; Lin & Lynden-Bell 1982; Gardiner et al. 1994; Gardiner & Noguchi 1996). In such models, orbits of the Large Magellanic Cloud (LMC) and the Small Magellanic Cloud (SMC) can be traced back in time over the entire past period of ~ 10 Gyr: The orbital plane is approximately perpendicular to the line joining the present position of the sun and the Galactic center, and they are viewed to move counterclockwise along a nearly great circle centered on $(l, b) = (0^\circ, 0^\circ)$ or the Galactic center.

However, the tidal model in which the Magellanic Clouds formed in the neighborhood of the Galaxy cannot explain large orbital angular momenta of the Magellanic Clouds around the Galaxy (see, for example, Fich & Tremaine (1994)). According to the theory of the Magellanic Stream, the apo-Galactic distance of the LMC orbit is $R_{\text{LMC}} \sim 200$ kpc and its transverse velocity is $V_{\text{LMC}} \sim 100 \text{ km s}^{-1}$ some 10 Gyr ago, implying that if the LMC mass is $M_{\text{LMC}} \sim 2 \times 10^{10} M_\odot$, the orbital angular momentum of the Magellanic Clouds L_{LMC} at that time is given by

$$\begin{aligned} L_{\text{LMC}} &\sim M_{\text{LMC}} R_{\text{LMC}} V_{\text{LMC}} \\ &\sim 2 \times 10^{10} M_\odot \times 200 \text{ kpc} \times 100 \text{ km s}^{-1} \\ &= 4 \times 10^{14} M_\odot \text{ kpc km s}^{-1}, \end{aligned} \quad (1)$$

while the spin of the Galactic disk L_{disk} in flat rotation with velocity V_0 is given by

$$L_{\text{disk}} \sim \int r V_0 dm$$

$$\begin{aligned} & \sim \int_0^{R_{\text{disk}}} \int_0^{2\pi} \int_{-h/2}^{h/2} \rho_0 r^2 V_0 dr d\phi dz \\ & = \frac{2\pi}{3} \rho_0 V_0 R_{\text{disk}}^3 h, \end{aligned} \quad (2)$$

where ρ_0 is the density of the disk, h the thickness, and R_{disk} the outer radius. In this estimate, we assume ρ_0 and h to be constant. Since the total mass of the disk M_{disk} is given by $M_{\text{disk}} = \pi R_{\text{disk}}^2 h \rho_0$, the spin of the Galactic disk L_{disk} is estimated as

$$\begin{aligned} L_{\text{disk}} & \sim \frac{2}{3} M_{\text{disk}} R_{\text{disk}} V_0 \\ & \sim \frac{2}{3} \times 2 \times 10^{11} M_{\odot} \times 15 \text{ kpc} \times 220 \text{ km s}^{-1} \\ & = 4 \times 10^{14} M_{\odot} \text{ kpc km s}^{-1}, \end{aligned} \quad (3)$$

if we adopt $V_0 = 220 \text{ km s}^{-1}$ and $M_{\text{disk}} = 2 \times 10^{11} M_{\odot}$ for $R_{\text{disk}} = 15 \text{ kpc}$. We find that the orbital angular momentum of the LMC, L_{LMC} , is comparable to the spin of the Galactic disk L_{disk} . It should be also born in mind that these angular momenta make a right angle against each other. They cannot be explained in terms of the tidal interaction in the LGG (Gott III & Thuan 1978). Further it has also been widely recognized that the morphological type of dwarf galaxies near their massive parent galaxy are generally dwarf spherical or spheroidal, but that the Magellanic Clouds are morphologically classified as dwarf irregulars in spite of their close location to the Galaxy and are exceptionally massive (Einasto et al. 1974) and gas-rich.

These facts are difficult to understand only in terms of the gravitational interaction among the three-body system, the Galaxy-LMC-SMC. Then Fujimoto et al. (1999) and Sawa et al. (1999) conducted numerical simulations of the Magellanic Stream by taking into account the gravitational effect of the nearby massive galaxy M31 which is approaching us with velocity of 120 km s^{-1} if we adopt the standard rotation velocity of the LSR ($V_0 = 220 \text{ km s}^{-1}$) and the solar motion ($v_{\odot} = 16.5 \text{ km s}^{-1}$, $l_{\odot} = 53^{\circ}$, $b_{\odot} = 25^{\circ}$). With the orbital elements of M31 assumed by Kahn & Woltjer (1959), Fujimoto et al. (1999), and Sawa et al. (1999), it is found that the binary orbits of the LMC and the SMC at their early times are much disturbed compared with those determined by Murai & Fujimoto (1980) and Gardiner et al. (1994), but no successful result has been obtained for solving the angular momentum problem even through the four-body dynamics of the Galaxy-M31-LMC-SMC.

The present authors come to take a view point that some questions about the Galaxy-LMC-SMC system must be answered through a more-global model for the LGG in which the Galaxy, the LMC and the SMC should be treated as three objects among more-than-forty members of the LGG. For this reason we begin with in the next section our reexamination of the sky (two-dimensional) and spatial (three-dimensional) distributions of the member galaxies of the LGG, which would give key ideas for the dynamics and the origin of the LGG.

In concluding this section, we note that many stud-

ies have tried to determine the past orbits of the LGG members under their various assumptions. They are conducted mostly in virial scheme and, therefore, the results are rather stochastic. Here we should refer to three important works by Mishra (1985), Peebles (1993), and Lynden-Bell (1999). They have pioneered the global LGG dynamics, although many basic differences are present from our ideas and results, particularly concerning the origin of the LGG.

2. Characteristic Distributions of the Local Group Dwarf Galaxies

2.1. Distributions of the LGG Members in the Galactic Coordinates

The concept of a Local Group of Galaxies was introduced as early as at the time of Hubble's distance and redshift measurements of extragalactic objects. The number of member galaxies of the Local Group has increased since that time and it is still so even at present. It is more than forty: See Mateo (1998) and van den Bergh (2000) for reviews of the LGG.

Figure 1 shows a sky distribution of the LGG members listed in the up-to-date table of Mateo (1998). The galactic coordinates (l, b) is adopted, but longitude/latitude grid-lines are ignored here in order to emphasize an impression that the LGG members are distributed not at random but in a somewhat systematic way forming a ring of large diameter of about 180° . The major axis of the sky rimmed with an ellipse is the Galactic plane, with $(l, b) = (180^{\circ}, 0^{\circ})$ at the both extreme ends, and the minor axis links the north and south Galactic poles. The Galactic center $(l, b) = (0^{\circ}, 0^{\circ})$ is located at the geometrical center of this ellipse.

If we exclude four dwarfs in the direction of the Galactic center, Sagittarius, SagDIG, NGC6822 and DDO210, the existence of the ring of $\sim 30^{\circ}$ in width appears to be more evident. The plane of the ring is perpendicular both to the Galactic plane and to the line joining the present position of the sun and the Galactic center. The apparently small tidal structure of the Sagittarius will be discussed later.

Such a ring-like distribution of the LGG dwarf galaxies and the Magellanic Stream was already pointed out in a few previous studies until the end of the 1970s, but it is widely considered to be rather accidental with no special meanings except some studies. As will be touched upon later, Kunkel (1979) claimed that the ring-like distribution of the Galaxy group dwarfs is an evidence for a big dynamical event which occurred in the neighborhood of the Galaxy some billion years ago and that a few dozen of proto-dwarf gaseous debris were driven to form and scatter on the plane as observed today in figure 1.

In order to emphasize the non-random distribution of dwarfs found in figure 1 more quantitatively, we draw in figure 2 two great circles and another great-circle-like line on the (l, b) plane. The dotted line is a great circle defined by twelve dwarf galaxies of the Galaxy group except Sagittarius which locates near the Galactic center, while the dashed line is that defined by the M31 group, i.e. M31

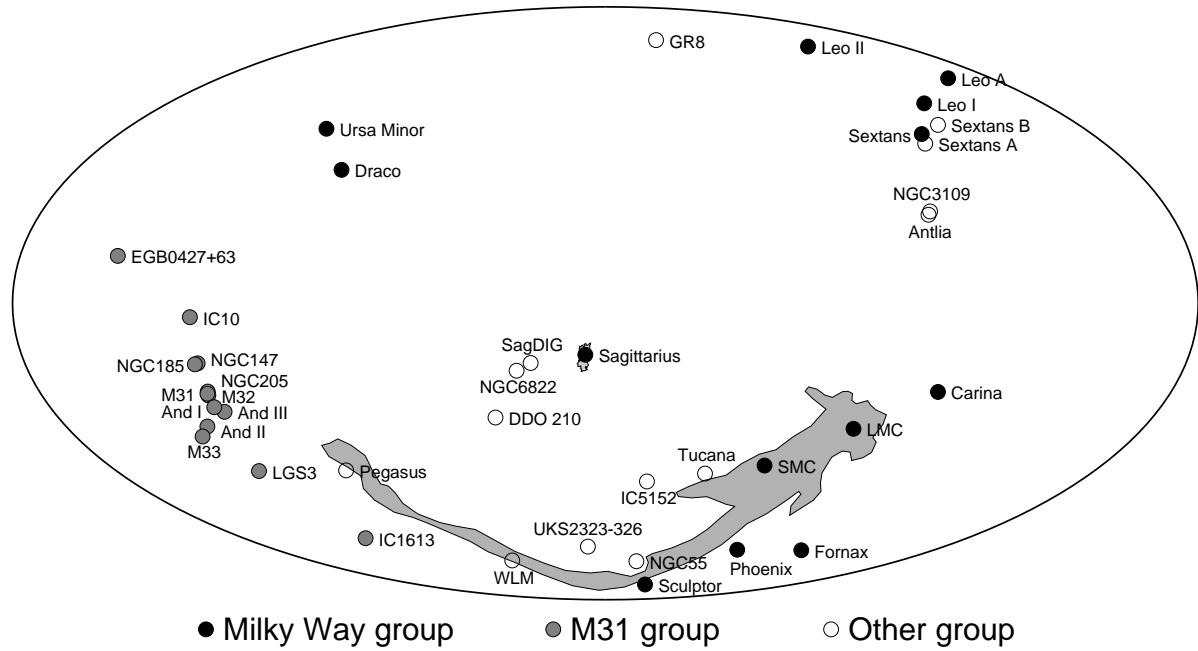


Fig. 1. Two-dimensional distribution of the members of the LGG and the Magellanic Stream in Hammer's projection onto the sky. The data are due to Mateo (1998), and the lines of the Galactic longitudes and latitudes are not given here in order to emphasize that these objects are distributed not in random but in some systematic way like in a ring of large diameter, except four dwarfs in the direction of the Galactic center. The filled circles indicate the Galaxy group members, the netted circles the M31 group and the open circles the nonparent group. Note that a tidal tail is sketched at the Sagittarius dwarf. Although it is very small, its major axis makes evidently a nearly right angle against the galactic plane.

and nine dwarfs. The great-circle-like solid line represents the last previous (~ 2 Gyr) orbit of the LMC projected onto the sky, which traces the Magellanic Stream. For the data of the LGG members, see Table 1.

These two great circles and another great-circle-like line (the LMC's orbit) do not coincide with each other exactly, but they occupy roughly a same half area of the sky. The existence of the ring-like structure suggested in figure 1 is considered as a result of superposition of these circles in figure 2.

The discordance among the three circles in figure 2, and the four dwarfs in the direction of the Galactic center in figure 1 will be taken into consideration in the framework of our LGG model presented later.

2.2. Three-Dimensional Space Distributions of the Local Group of Galaxies

Figures 1 and 2 give only distribution of the LGG dwarfs projected onto the sky planes, lacking the information on the distance measured on the line-of-sight. We plot the positions of the LGG members (Table 1) in the three-dimensional rectangular coordinates and see them from various directions. Such analyses have been made in many other previous studies, and are known to be convenient to obtain an overview about the LGG structure because we can avoid the large parallaxes of the members which are located close to the Galaxy. The dwarf galaxies in the

Sagittarius region, which are discarded in our discussions about the ring structure in figures 1 and 2, are this case. See Majewski (1994), Mateo (1998), Lynden-Bell (1999), and van den Bergh (2000) for their review articles about the three-dimensional structure of the LGG.

Figure 3 shows a distribution of the LGG members seen from the direction $(l, b) = (296^\circ, -11^\circ)$. There can be seen clear alignment along the line passing M31 and the Galaxy; the LGG members are distributed in a coplanar way or in a flat disk of finite thickness of 50-100 kpc, which makes the ring-like or circle-like distributions of the LGG members in figures 1 and 2. The disk plane is approximately perpendicular to the direction toward $(l, b) = (0^\circ, 0^\circ)$, and/or the Galactic center.

Three objects shown by open circle locate 200-300 kpc apart from the disk plane. Compared with the radius of the LGG of 1Mpc (Lynden-Bell 1999), such separation is not so large, and hence we think that they also contribute to defining the LGG plane. Other two objects, EGB0427+63 and Leo A, are exceptionally distant from the disk plane; they may be intruders (see later).

Hartwick (2000) analyzed the 3-dimensional positions of the LGG members and determined the spheroidal distribution for the Galaxy group members and the M31 group ones, respectively. He pointed out that the disk plane of these two spheroids are nearly parallel, but make a small angle between them. Indeed, if we observe figure 3 from

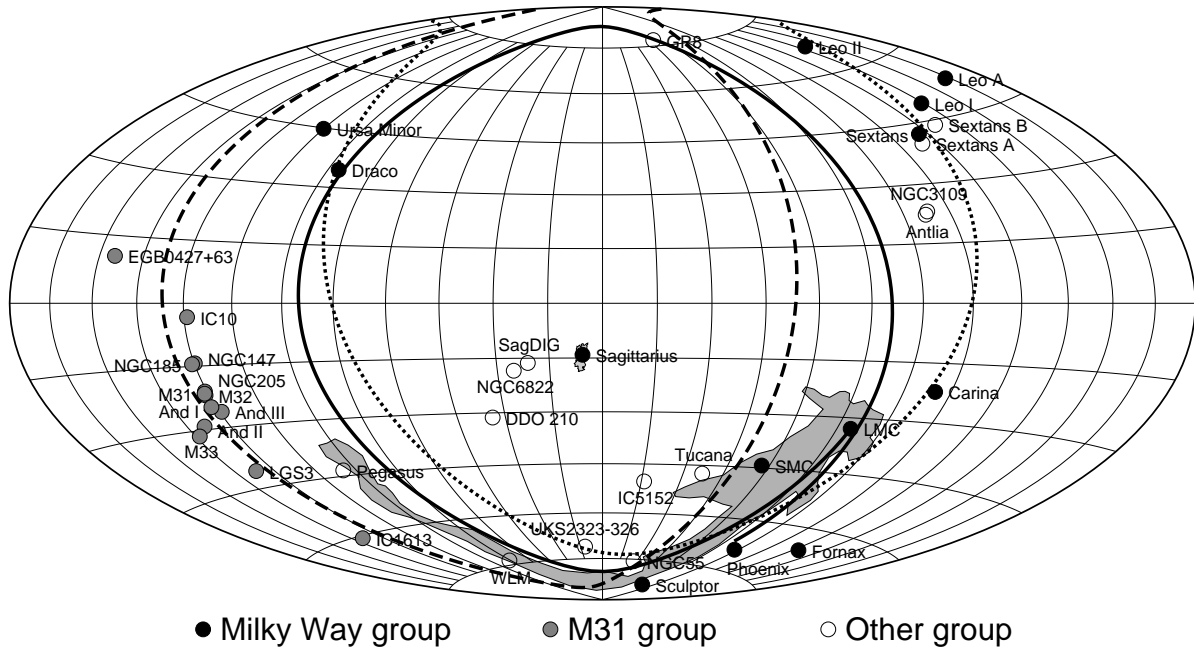


Fig. 2. Two great circles in dashed and dotted lines and another circle in solid line on the (l, b) -plane of the sky. The constant lines of the Galactic longitude and latitude (l, b) cover all the same sky as in figure 1. The dotted line indicates a great circle fitted to the distribution of the Galaxy group members, the dashed line to that of the M31 group members and the solid line traces a last revolution orbit of the LMC about the Galaxy (Gardiner et al. 1994). These three circles occupy approximately the same large area of the sky, suggesting the existence of the ring-like sky distribution of the LGG members, although the angle discordance of $\sim 30^\circ$ in maximum is recognized among these circles.

a slightly different view-direction, the Galaxy members align more clearly and those of the M31 group are a little more dispersed.

Although such structure difference may indicate some special initial condition for the LGG dynamics (Hartwick 2000), we ignore it here and construct a dynamical model for the LGG. Hartwick's fine structure will be considered in another paper as a first-order perturbation to our LGG model. Then, Raychaudhury and Lynden-Bell's dynamics (Raychaudhury & Lynden-Bell 1989) may give us a new hint to this problem that the tidal torque due to nearby massive galaxies outside the LGG region would have perturbed the motions of M31, the Galaxy and their dwarfs over the past 10^{10} years.

Figure 4 represents a 3-dimensional distribution of the LGG members viewed from the direction $(l, b) = (206^\circ, -11^\circ)$, normal to the plane identified in figure 3. We call it a *face-on view* against the plane of the LGG, and then figure 3, an *edge-on view* against the LGG disk. Even in the face-on view, the LGG members are distributed not in random but in a systematic way, as grouped around M31 and the Galaxy, respectively.

Dwarf galaxies of open circles gather around neither M31 nor the Galaxy. They appear to link these two mass-dominant galaxies, suggesting that M31 and the Galaxy interacted strongly at their early ages. However, we note that these dwarfs are not confined exactly in the LGG disk

(the plane of this page) of finite thickness but are apart from it with some distance.

3. A Dynamical Model for the Local Group of Galaxies

The ring-like or circular distributions of the LGG members on the sky (figures 1 and 2) are consistent with the existence of the LGG disk with finite thickness of 50-100 kpc (figures 3 and 4).

As briefly touched upon in section 2, Kunkel (1979) considered that a destructive dynamics occurred some billion years ago in the space near the Galaxy and a dozen of gaseous debris were generated to move around it. The ring-like sky-distribution of the dwarf galaxies is just a result of a view from inside of the Galaxy. We now extend Kunkel's idea (Kunkel 1979) to an earlier and larger-scale dynamics related to the whole LGG structure. The data are due exclusively to figures 1 to 4.

An up-scaled model for the LGG dynamics is as follows. Seen from the Galaxy, early still-extended gas-rich M31 encountered the early similar Galaxy at the perigalacticon of ~ 150 kpc about 10 Gyr ago. (These numerical values are to be determined through constructing the model quantitatively in the next section.) The M31 orbit is an unclosed elliptical, and M31 leaves the Galaxy until it reaches the apogalacticon at ~ 1 Mpc about 4 Gyr ago

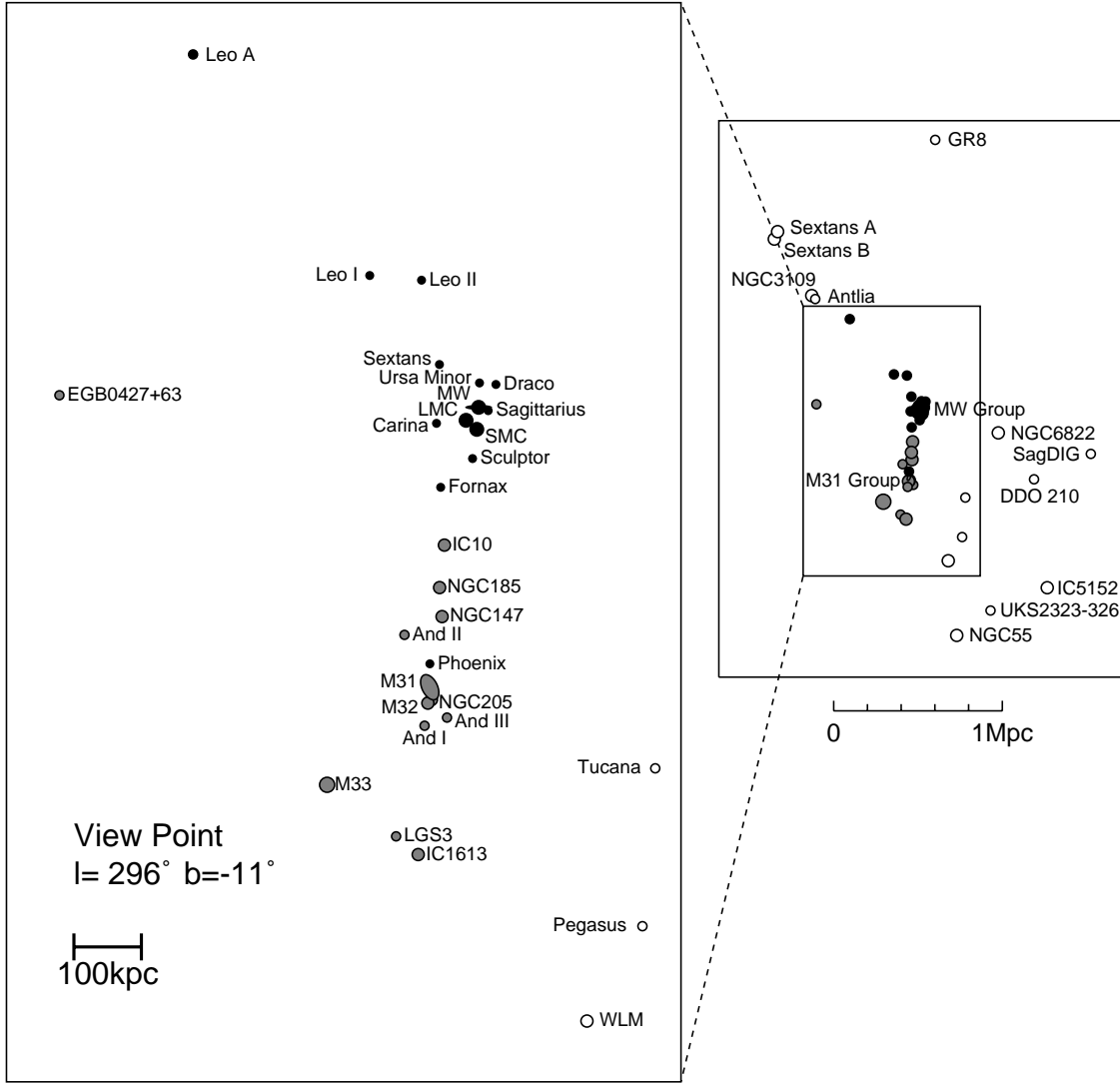


Fig. 3. Three-dimensional space distribution of the LGG members, seen from the direction $(l, b) = (296^\circ, -11^\circ)$. This is an *edge-on* view of the orbital plane of the Galaxy and M31. The perspective representation is not applied. The filled circles denote the Galaxy group members, the netted ones the M31 group members and the open ones the members that belong neither to the Galaxy nor to M31. We recognize that the LGG members are distributed in a flat disk of finite thickness of 50-100 kpc. The size of each circle represents its brightness only qualitatively. Note that some number of dwarf galaxies are not given on the outside of the LGG region whose radius is ~ 1 Mpc. They are plotted in the inset on upper-right, together with all galaxies listed in the Table 1.

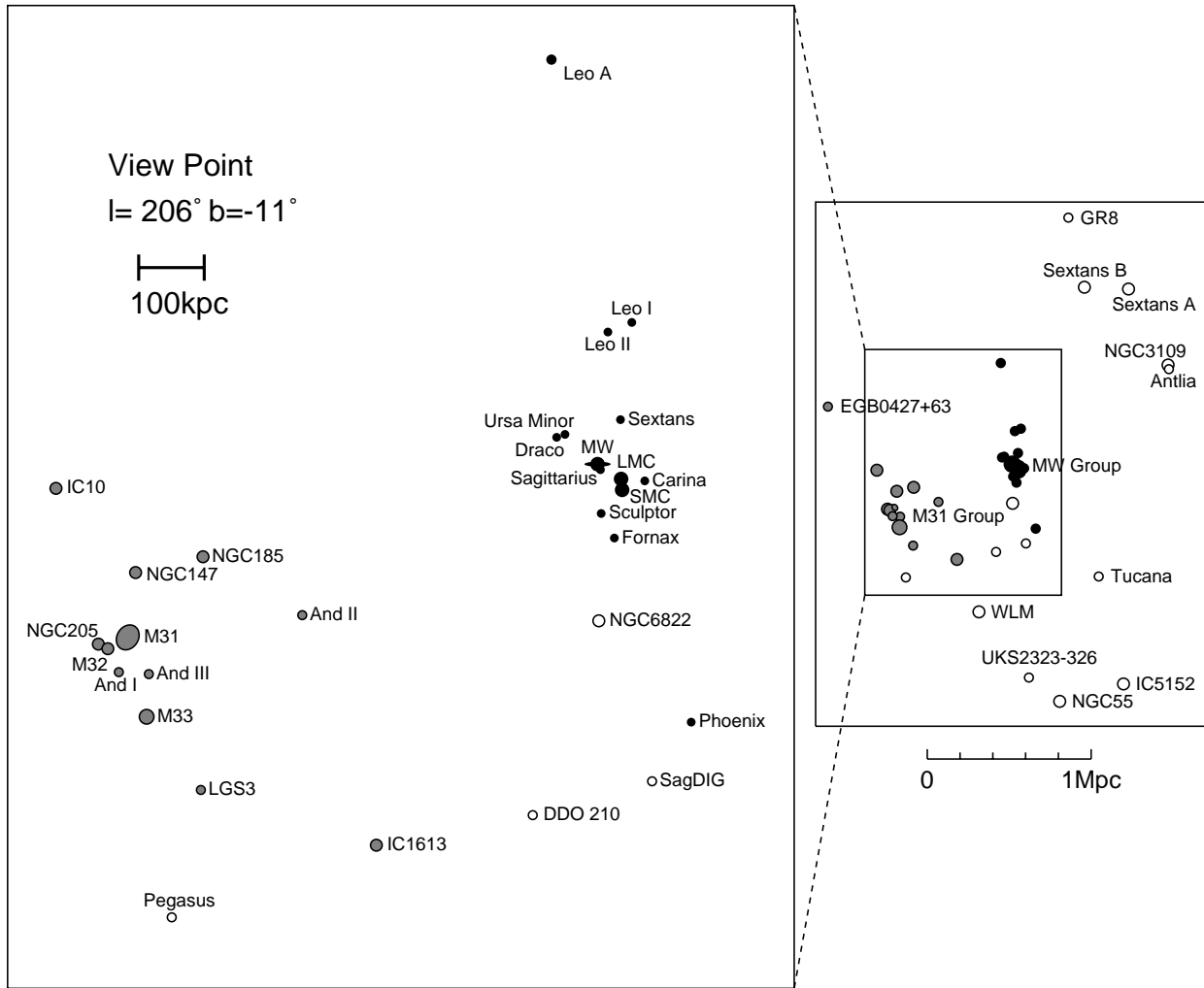


Fig. 4. The same as in figure 3, but seen from the direction $(l, b) = (206^\circ, -11^\circ)$. This is a *face-on view* of the LGG plane, or of the orbital plane of the Galaxy and M31 in the present model. The Galaxy group and the M31 group members, and nongroup members appear to form a fragmentary ring whose diameter is ~ 800 kpc and more. We note that some of the nongroup members, Pegasus, DDO210, SagDIG and NGC6822 are not exactly in the LGG plane of finite thickness. They are located off from the plane by 160-730 kpc, large compared with the disk thickness, but small compared with the LGG's radius of ~ 1 Mpc. They also contribute to forming our model of the coplanar structure of the LGG. The inset on upper-right is the same as that in figure 3, but viewed face-on.

Table 1. Applied Parameters for the Local Group of Galaxies*.

Galaxy Name	Other name	<i>l</i>	<i>b</i>	<i>r</i>	<i>v_r</i>	Group
WLM	DDO 221	75.9	-73.6	925	-123	LGC
NGC55		332.7	-75.7	1480	124	LGC
IC10	UGC192	119.0	-3.3	825	-342	M31
NGC147	DDO3	119.8	-14.3	725	-193	M31
And III		119.3	-26.2	760	—	M31
NGC185	UGC396	120.8	-14.5	620	-204	M31
NGC205	M110	120.7	-21.1	815	-229	M31
M32	NGC221	121.2	-22.0	805	-197	M31
M31	NGC224	121.2	-21.6	770	-297	M31
And I		121.7	-24.9	805	—	M31
SMC	NGC292	302.8	-44.3	58	148	MW
Sculptor		287.5	-83.2	79	102	MW
LGS3	Pisces	126.8	-40.9	810	-272	M31
IC1613	DDO8	129.8	-60.6	700	-234	M31/LGC
And II		128.9	-29.2	525	—	M31
M33	NGC598	133.6	-31.3	840	-181	M31
Phoenix		272.2	-68.9	445	56	MW/LGC
Fornax		237.1	-65.7	138	53	MW
EGB0427+63	UGCA92	144.7	+10.5	1300	-87	M31
LMC		280.5	-32.9	49	274	MW
Carina		260.1	-22.2	101	224	MW
Leo A	DDO69	196.9	+52.4	690	26	MW/N3109
Sextans B	DDO70	233.2	+43.8	1345	303	N3109
NGC3109	DDO236	262.1	+23.1	1250	404	N3109
Antlia		263.1	+22.3	1235	361	N3109
Leo I		226.0	+49.1	250	286	MW
Sextans A	DDO75	246.2	+39.9	1440	325	N3109
Sextans		243.5	+42.3	86	277	MW
Leo II	DDO93	220.2	+67.2	205	76	MW
GR8	DDO155	310.7	+77.0	1590	215	GR8
Ursa Minor	DDO199	105.0	+44.8	66	-248	MW
Draco	DDO208	86.4	+34.7	82	-293	MW
Milky Way		0.0	0.0	8.5	—	MW
Sagittarius		5.6	-14.1	24	140	MW
SagDIG	UKS1927-177	21.1	-16.3	1060	-79	LGC
NGC6822	DDO209	25.3	-18.4	490	-54	LGC
DDO 210	Aquarius	34.0	-31.3	800	-137	LGC
IC5152		343.9	-50.2	1590	124	LGC
Tucana		322.9	-47.4	880	—	LGC
UKS2323-326	UGCA 438	11.9	-70.9	1320	62	LGC
Pegasus	DDO216	94.8	-43.5	955	-182	LGC

*) Due principally to Mateo 1998, but the radial velocities of the LMC and the SMC are to Tully 1988.

Galaxy Name: Names of the Members of the Local Group of Galaxies. Other name: Other names of the applied members.

l: The Galactic longitude in degree.

b: The Galactic latitude in degree.

r: Distance from the sun measured in kpc.

v_r: Heliocentric radial velocity in km s⁻¹.

Group: Name of galaxy group, to which the above members belong. MW means the Milky Way, M31 the Andromeda galaxy.

and then starts to approach the Galaxy.

At this early off-center collision, the still-extended gas of the Galaxy and that of M31 compresses each other hydrodynamically to generate a high density region of gas at a half way between them. A number of gas clouds are driven to condense and scattered on the orbital plane. Some tens of them evolved into dwarf galaxies as we now observe them. Most of these dwarfs gather gravitationally around the Galaxy or M31, and other several ones are left behind from such groupings, belonging neither to the Galaxy nor to M31. In our model, the orbital plane of the Galaxy-M31 is assumed to be identical with the LGG disk, determined in figure 3, or with the plane defined by the rings in figures 1 and 2.

In this connection, we refer to Deeg et al. (1998), in which the violently merging gas-rich galaxies are observed just like shedding out a number of young dwarf galaxies around them. These authors claim that a considerable portion of the observed dwarf galaxies are not cosmological objects but recently born ones in and around the interacting galaxies. A recent HST observation by Weaver et al. (2001) reveals clearly that the disk galaxy NGC7318 in the Stepfan's Quintet is generating dozens of dwarf galaxies in tidal interaction with its nearby galaxy. These dwarfs appear to distribute dominantly on an orbital plane of NGC7318 and its counterpart. Our LGG model can be, therefore, regarded as an earlier and larger-scaled version of these interacting galaxies and newborn dwarfs around

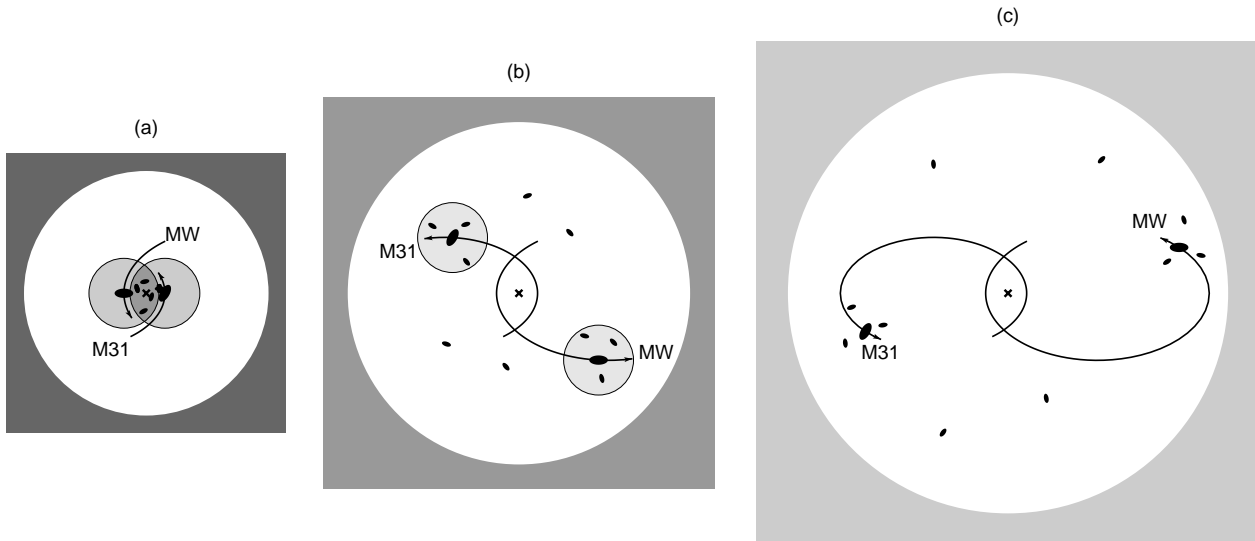


Fig. 5. Schematic snapshots of the dynamical evolution of the LGG members in local cosmic expansion. Figures 5(a) to 5(c) are face-on views of the LGG disk and one of which, figure 5(c), corresponds to figure 4. A visual explanation is given for determining the orbits of M31 and the dwarf members. The radii of the LGG spherical regions and the darkness around them represent the expanding universe seen in local, and the cross denotes the center-of-mass of the Galaxy and M31. (a): 12 to 10 Gyr ago. The gas-rich proto-Galaxy and the similar proto-M31 approach each other along their elongated orbits, making an off-center collision to compress their halo gasses hydrodynamically. The early dwarfs, including the LMC and the SMC, are driven to form there. This high-density region is approximated geometrically to an overlapped area of the large halo spheres of the early Galaxy and M31. Since it is colored in dark gray in figure 5(a), it is referred to in the text as a *gray area*, and sometimes as (halo) *overlapped region*, (gas) *compressed region*, (dwarf) *formation site*, etc. (b): ~ 8 Gyr ago. The newborn dwarf galaxies are scattered on the orbital plane of the Galaxy and M31. After 4 Gyr of this epoch, the Galaxy and M31 pass their apogalacticons at a distance of 1 Mpc from each other, and start approaching. Some dwarf members are already partitioned into the neighborhoods of the Galaxy and M31. (c): At present. M31 is at 770 kpc from the Galaxy and approaching us with radial velocities of 120 km s^{-1} . This figure suggests the existence of the azimuthal motion of M31 relative to the Galaxy.

them.

Figures 5(a) to 5(c) are given to explain visually our model for the LGG origin and evolution. A spherical outer surface of the LGG region and the darkness outside it mimic the expansion of the universe seen in the local coordinates. The mass in this sphere is assumed to have condensed exclusively to two mass-dominant galaxies, the Galaxy and M31, and two massive dwarfs, the LMC and the SMC. Other dwarfs including M33 are treated as test particles which move in time-dependent gravitational potential due to the above four galaxies in the expanding sphere.

Since the radiation energy is far less than the rest mass energy in our cosmological space and time, this spherical surface of R in radius follows (Landau & Lifshitz 1975),

$$R = R_0(1 - \cos \eta), \quad (4)$$

and

$$t = t_0(\eta - \sin \eta), \quad (5)$$

for closed universe, and

$$R = R_0(1 - \cosh \eta), \quad (6)$$

and

$$t = t_0(\eta - \sinh \eta), \quad (7)$$

for open universe, and

$$R \propto t^{2/3} \quad (8)$$

for flat universe, where R_0 and t_0 are constants and η is a parameter. In the present paper, we adopt equation (8), although choice of the universe is not crucial on our discussion for the dynamics of the LGG members. The dark energy that could accelerate the Hubble expansion unnegligibly in this 4 Gyr is not taken into account for simplicity. Also we ignore the distortion of the spherical surface of the LGG region, because the perturbing force due to the gravitational quadrupole moment of the LGG members decays quickly as $1/R^3$.

In figure 5(a) early gas-rich M31 and the similar Galaxy approach each other, and subsequently hydrodynamic off-center collision occurred between them to generate a high-density region of gas where a number of gas clouds, which include the proto-LMC and the prot-SMC, form. The collision epoch is ~ 10 Gyr ago. This region is modeled in the present paper by a geometrically overlapped area of the early-large-sized Galaxy and the similar M31. It will be referred to hereafter as an *overlapped region*, (hydrodynamically gas) *compressed region*, (dwarf) *formation site*, etc. In figures 5(b) and 5(c), the primordial dwarf galaxies scatter mostly on the orbital plane of M31

and the Galaxy, and each evolves to the dwarf members as observed presently. More exactly they move in the gravitational potential due to the Galaxy, M31, the LMC and the SMC. The orbital plane of the Galaxy and M31 in figures 5(a) to (c) is taken to be the same as this page, and the newborn dwarfs distribute approximately on this plane with small but finite thickness. In concluding this section, we note a CDM universe which is assumed implicitly in our model. According to this widely-accepted theory, cosmologically large-scale structures are considered to have grown from primordial density-fluctuations of baryonic and dark matters, whose square of amplitude is distributed in inverse law of the wave number. We can suppose naturally that the corresponding random motion was superposed on the Hubble expansion flow, and its amplitude is also in a power-law function of the wave number. The LGG dynamics that we have modeled in the present paper is consistent with such a CDM universe. That is, the proto-Galaxy and proto-Andromeda were formed from such baryonic and dark matter media in various vortices. Their early off-center collision is considered to occur in a finite probability.

4. Orbital Motions of M31 and the Galaxy Over the Past 12 Gyr, Determined from the LMC/SMC Dynamics

We now construct a LGG model quantitatively following figures 5(a) to (c). First we survey numerically past orbits of M31 by fixing its radial velocity as that in Table 1 and varying its tangential velocities which are still unknown. Then we choose most reasonable orbits which satisfy our criteria that the orbital plane lies within the LGG disk of finite thickness (figure 3), and M31 was close to the Galaxy at a cosmologically early epoch. The latter criterion is required for the early collision between primordial M31 and the primordial Galaxy, and it means that these two galaxies had deviation from Hubble expansion law, as stated above. Such picture of the universe is quite different from those adopted in previous studies (Mishra 1985; Peebles 1993; Lynden-Bell 1999) where all LGG members are assumed to follow initially the Hubble expansion, starting from a single region of finite but small size.

The off-center collision compresses the halo gas hydrodynamically to generate a high density region at a half way between the primordial M31 and Galaxy at their closest approach. Figure 5(a) shows that primordial dwarfs, including the primordial LMC and SMC, form in this region and scattered roughly on the Galaxy-M31 orbital plane, in the same direction as the M31 motion seen from the Galaxy.

We adopt a reasonable assumption that the LMC/SMC thus formed have been in a binary state for the past ~ 10 Gyr and produces the Magellanic Stream. In other words, the LMC/SMC structure is a key phenomenon for determining the dynamical parameters of the Galaxy-M31 orbit and of the LGG model numerically. Simultaneously if our model proves realistic, one of our basic questions about

the large orbital angular momentum of the LMC/SMC is answered automatically.

The overall dynamical structure and evolution for other dwarfs of the LGG will be discussed in the next section. See Hodge (1992) for the details of M31, and Westerlund (1997) for the dynamics and physics of the LMC/SMC system.

In applying the four-body dynamics to the Galaxy, M31, the LMC and the SMC, we adopt the following parameters. We assume that M31 and the Galaxy have a dark halo each with radius of 300 kpc and that the rotation curve is flat in both galaxies. Then, the total gravitating mass of M31, including dark halo mass, is $M_A = 4 \times 10^{12} M_\odot$ for the rotation velocity $V = 250 \text{ km s}^{-1}$, and that of the Galaxy is $M_G = 3 \times 10^{12} M_\odot$ for $V = 220 \text{ km s}^{-1}$. Note that we are rediscussing the masses of M31 and the Galaxy in section 7.

M31 is located at 770 kpc of the sun in the direction of $(l, b) = (121^\circ, -22^\circ)$. The heliocentric radial velocity of M31 is -298 km s^{-1} (Tully 1988), which corresponds to the radial velocity of -120 km s^{-1} relative to the Galactic center. The masses of the LMC and the SMC are taken to be $2 \times 10^{10} M_\odot$ and $2 \times 10^9 M_\odot$, respectively, which have been applied in models by Murai & Fujimoto (1980) and Gardiner et al. (1994). Numerical values for all other parameters are conventional and the same with those applied in the four-body dynamics in Fujimoto et al. (1999) and Sawa et al. (1999).

We follow the orbits of M31, the LMC, and the SMC (relative to the Galaxy) backward in time from present to the beginning of the universe, 10-13 Gyr ago, as schematically shown in the “expanding” (or exactly, “shrinking,” because we follow the dynamics backward in time) LGG sphere in figures 5(a) to 5(c). For calculation of the orbits, we assume various tangential components of the velocity of M31 (V_l, V_b) in the Galactic longitude and latitude. We take the following four conditions (i) to (iv) all of which should be satisfied in reasonable cases and also in order to restrict the values of (V_l, V_b) within some limited ranges beforehand. (i) The primordial M31 passes by the primordial Galaxy at their cosmologically early age, say, 9 to 13 Gyr ago. (ii) The orbit of M31 is roughly on the plane determined in figure 3. In this case the nodal line links the Galactic center and the present position of M31. (iii) M31 orbits the Galaxy counterclockwise seen from the present position of the sun, in the same sense as the LMC/SMC. (iv) The LMC and the SMC pass computationally through the gray petal-like region located midway between the primordial M31 and Galaxy in figure 5(a). The passage must be at the same time when this hydrodynamically-compressed region is formed.

We apply the following equation (9) to our tracing back-in-time the Andromeda galaxy (M31), supplemented with other three similar equations (10) to (12) for the Galaxy, the LMC and the SMC;

$$M_A \ddot{\mathbf{r}}_A = -\frac{\partial \phi_G}{\partial \mathbf{r}_A} - F_A^G \frac{\dot{\mathbf{r}}_A - \dot{\mathbf{r}}_G}{|\dot{\mathbf{r}}_A - \dot{\mathbf{r}}_G|}, \quad (9)$$

$$M_G \ddot{\mathbf{r}}_G = -\frac{\partial \phi_A}{\partial \mathbf{r}_G} - F_G^A \frac{\dot{\mathbf{r}}_G - \dot{\mathbf{r}}_A}{|\dot{\mathbf{r}}_G - \dot{\mathbf{r}}_A|}, \quad (10)$$

$$\begin{aligned} M_L \ddot{\mathbf{r}}_L &= -\frac{\partial}{\partial \mathbf{r}_L} (\phi_A + \phi_G + \phi_S) \\ &- F_L^A \frac{\dot{\mathbf{r}}_L - \dot{\mathbf{r}}_A}{|\dot{\mathbf{r}}_L - \dot{\mathbf{r}}_A|} - F_L^G \frac{\dot{\mathbf{r}}_L - \dot{\mathbf{r}}_G}{|\dot{\mathbf{r}}_L - \dot{\mathbf{r}}_G|}, \end{aligned} \quad (11)$$

and

$$\begin{aligned} M_S \ddot{\mathbf{r}}_S &= -\frac{\partial}{\partial \mathbf{r}_S} (\phi_A + \phi_G + \phi_L) \\ &- F_S^A \frac{\dot{\mathbf{r}}_S - \dot{\mathbf{r}}_A}{|\dot{\mathbf{r}}_S - \dot{\mathbf{r}}_A|} - F_S^G \frac{\dot{\mathbf{r}}_S - \dot{\mathbf{r}}_G}{|\dot{\mathbf{r}}_S - \dot{\mathbf{r}}_G|}, \end{aligned} \quad (12)$$

where the geometrical and dynamical symbols with suffices A, G, L and S are referred to those of the Andromeda (M31), the Galaxy, the LMC and the SMC, respectively. The gravitational potentials ϕ_i ($i = A, G$) are given by the potential for the flat rotation, and those ($i = L$ and S) are softened conventionally by introducing their central cores of finite radii. The dynamical frictions, given by the extremely-right ends of equations (9) to (12) are due primarily to the extended halos of the M31 and the Galaxy. The two factors in equations (11) and (12), (F_L^A, F_L^G) and (F_S^A, F_S^G), denote the frictions on the LMC and the SMC due to the halos of M31 and the Galaxy. No frictions are considered between the LMC and the SMC. The adopted frictions F_i^j ($i = A, G, L, S$, and $j = A, G$) are as follows (Binney & Tremaine 1987):

$$F_i^j = -\frac{GM_i^2 \ln \Lambda}{|\mathbf{r}_i - \mathbf{r}_j|^2 X_j^2} \left\{ \operatorname{erf}(X_j) - \frac{2X_j}{\sqrt{\pi}} \exp(-X_j^2) \right\} \quad (13)$$

where $X_j = |\dot{\mathbf{r}}_i - \dot{\mathbf{r}}_j|/V_{j0}$, and V_{j0} of $j = A$ and G are the flat rotation velocities of the Andromeda galaxy and the Galaxy. The $\ln \Lambda$ is the Coulomb logarithm for the gravitational force and we use the value $\ln \Lambda = 3.0$ in our simulations. The other notations denote their usual meanings.

Figure 6 shows the tangential velocities (V_l, V_b) , in the extensive range of $-500 \text{ km s}^{-1} \leq V_l \leq 500 \text{ km s}^{-1}$ and $-500 \text{ km s}^{-1} \leq V_b \leq 500 \text{ km s}^{-1}$, adopted in our backward search of the M31 orbits that satisfy the above four conditions (i) to (iv). The orbits, computed from the tangential velocities in the upper- and lower-opened wedges of (V_l, V_b) , are confined within $\pm 30^\circ$ about the plane normal to the line joining the Galactic center and the present position of the sun, and then the nodal line links the Galactic center and the present position of M31. In particular, the M31 orbits in the lower wedge of figure 6 satisfy the conditions (ii) and (iii), and those of the filled circles produce the model orbits which pass the peri-Galacticon of 140 kpc about 10 Gyr ago at the same time when the Magellanic Clouds System goes through just this midway between M31 and the Galaxy. This dynamics is consistent with the condition (iv). It is easily seen that if the conditions (ii) to (iv) are satisfied, the condition (i) is automatically so.

As mentioned in the caption of figure 6, we can choose the tangential velocity $(V_l, V_b) = (140 \text{ km s}^{-1}, -180 \text{ km s}^{-1})$ marked with double circle as the most probable or

the most realistic value among five filled circles. The corresponding proper motion is, if observed in near future, $(\mu_l, \mu_b) = (38 \mu\text{as yr}^{-1}, -49 \mu\text{as yr}^{-1})$. It is noted that the conversing point of the radial lines $(V_l, V_b) = (130 \text{ km s}^{-1}, -80 \text{ km s}^{-1})$ in figure 6 is due to the vectorial summation of the Galactic rotation and the solar motion.

The most probable model orbits, projected onto the LGG plane are shown in figure 7. There can be seen that the orbital plane of M31 coincides approximately with that of the LMC/SMC system, and M31 makes an off-center collision with the Galaxy. A large-scale compression of primordial gas seems to be realized. The epoch of the collision is determined as 10.4 Gyr ago. Moreover importantly, the LMC/SMC also pass across this region 10.4 Gyr ago; the motions of M31 and the LMC/SMC thus lend a support to our model idea that primordial dwarfs, including the LMC and the SMC, were driven to form in the high density region of gas. Only a small portion of the orbital angular momentum of M31 (around the Galaxy) is transferred to those of the LMC/SMC simultaneously.

The orbits of M31, the LMC and the SMC over the past 12 Gyr are shown in figure 8, projected onto the (l, b) plane. Note that the orbits of the LMC and the SMC earlier than 10.4 Gyr do not concern our model construction. A comparison with figures 1 and 2 presents actually a two-dimensional coincidence between the model orbits and the rings or circles which trace the sky distribution of the LGG members. The perigalacticon of the M31 orbit is in the direction of $(l, b) = (307^\circ, 34^\circ)$, and the apogalacticon in $(119^\circ, -1^\circ)$. Their distances, measured from the Galactic center, are respectively 140 kpc and 980 kpc. The formation site of the LMC/SMC is near in the direction of the perigalacticon. Of course, this region is also the formation site of the LGG dwarfs as shown in gray in figure 5(a).

The orbits and attached numerals in figures 7 and 8 are more-or-less variable depending on the numerical values for the parameters of the LGG and the age of the universe. However, so far as they change only within some reasonable ranges, the overall features of the orbits of M31 and those of the LMC and the SMC remain essentially unchanged. For future studies of the LGG, therefore, it would be useful to predict again here numerically the proper motions of M31,

$$(\mu_l, \mu_b) = (38 \pm 16 \mu\text{as yr}^{-1}, -49 \pm 5 \mu\text{as yr}^{-1}). \quad (14)$$

Here we may not understand why the proper motion μ_l is comparable to μ_b in magnitude, because the orbital plane of M31 has been determined as nearly perpendicular to the Galactic plane. To this question, we recall that the transverse velocity to be observed is contributed from the Galactic rotation of 220 km s^{-1} , directed off from M31 by more than 30° .

5. Origin and Dynamics of Dwarf Members of the LGG

In our LGG model, the dwarf members, including the LMC and the SMC, are driven to form in the high-density

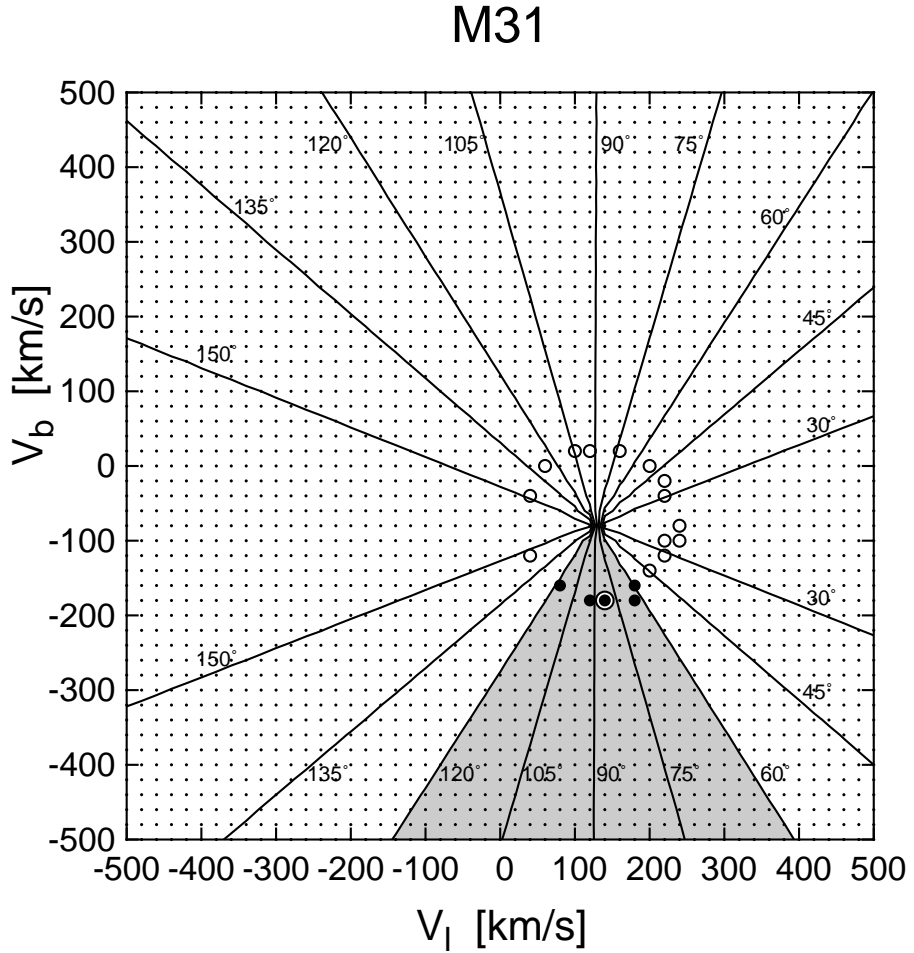


Fig. 6. Tangential velocities of M31 (V_t, V_b) assumed for tracing its past orbits. Model orbits of M31, computed with the tangential velocities of open and filled circles, can reproduce the dynamics that the LMC/SMC system was driven to form in the gray area in figure 5(a), and has been in a binary state for this 10^{10} yr, reproducing the Magellanic Stream through particle simulations. Other velocities of small dots cannot reproduce these dynamics. Roughly-radial contour lines indicate the angle between the orbital angular momentum of M31 and the direction of the Galactic north pole (z axis). If we apply the tangential velocities (V_t, V_b) shown by filled circles in the lower shaded region, the orbit of M31 is in the LGG disk of finite thickness, and one of the most representative tangential velocities are at a double circle $(V_t, V_b) = (140 \text{ km s}^{-1}, -180 \text{ km s}^{-1})$. The corresponding proper motion is $(\mu_t, \mu_b) = (38 \mu\text{as yr}^{-1}, -49 \mu\text{as yr}^{-1})$.

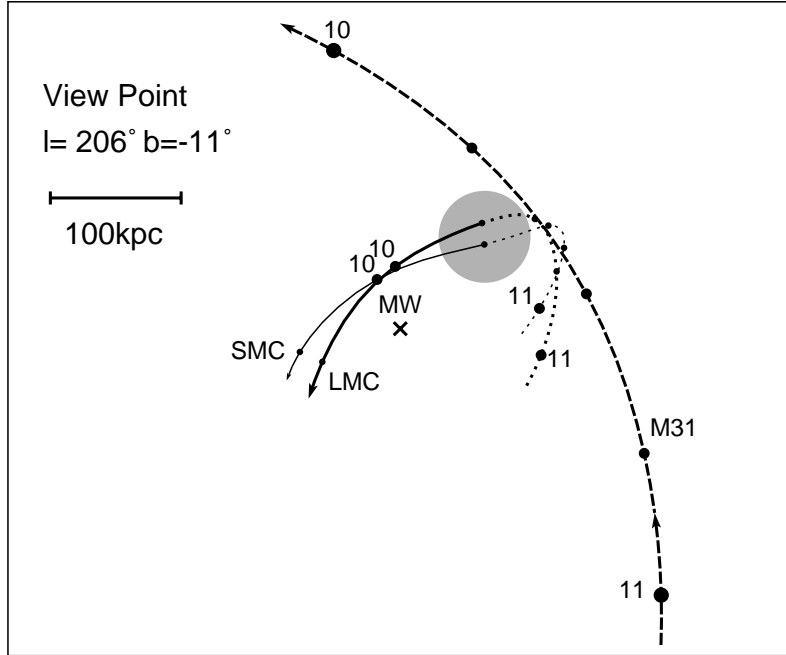


Fig. 7. Time-, position- and direction-matching between the cosmologically early orbits of M31 and that of the LMC/SMC on the LGG plane. It is viewed from the same direction of figure 4 or $(l, b) = (206^\circ, -11^\circ)$. They are given relative to the Galaxy (the cross at center). In order to avoid confusion, the orbits later than 10 Gyr are not given. The orbital planes of M31 and the LMC/SMC are nearly on this page. The arrows indicate the direction of motion toward the present and the attached numerals indicate the time in 1 Gyr measured from the present. The gray region denotes a formation site of the LMC/SMC system. Since the orbits of the LMC/SMC before entering this region do not concern the present model, we show them only in dotted lines in order to see how they are matched with the M31 orbit in position, time and velocity.

region of gas generated by the ancient off-center collision between M31 and the Galaxy. Newborn dwarf-galaxies are scattered approximately on the orbital plane of these two massive galaxies, and move in the time-dependent potential due mostly to the Galaxy and M31. The grown-up dwarfs tend to gather around either the Galaxy or M31, with minor ones left behind from such groupings. They are observed in the space between M31 and the Galaxy as if connecting geometrically these two galaxies (figures 3 and 4).

In order to check the validity of our model, we here examine whether or not the dwarf members in figure 3 and Table 1 have their past orbits which are consistent with our model scenario.

Exactly in the same way as for the case of the past orbits of the LMC and the SMC, we trace back in time the dwarfs' orbits from their present positions, with observed radial velocities (Table 1) and tangential velocities assumed on the (V_l, V_b) plane as in figure 6. Again the time-dependent gravitational potential due to the Galaxy, M31, the LMC and the SMC is adopted, and the latter two objects are required to be in a binary state for the past 10^{10} yr and to reproduce the geometrical and dynamical structures of the Magellanic Stream through the particle simulation.

We have thus surveyed computationally all past orbits

of the dwarf members in Table 1, and examined if they pass across the overlapped region of the primordial Galaxy and the primordial M31 ~ 10.4 Gyr ago (figure 7). Note that the dwarfs with no available data on radial velocities in Table 1 are excluded from our orbit computations.

Figure 9 shows an orbit of the LGG dwarf spheroidal, Draco (Dsp), which is presently at $(l, b) = (86.4^\circ, 34.7^\circ)$ and 82 kpc distant from the sun (Table 1). We can see that the orbit starts from the same formation site as that for the LMC/SMC, and arrives at the present position of the Draco.

The orbit has been determined by assuming a proper motion on the (V_l, V_b) plane in figure 10, where each symbol has the same meaning as that in figure 6, but nearly radial contour-lines indicate that (V_l, V_b) on these lines guarantee respectively same angles between the orbital plane of the Draco and that of the Galaxy-M31 system. The present proper motion (μ_l, μ_b) predicted for the Draco in Table 2, is based on the orbit determined with the velocity (V_l, V_b) at the double circle in figure 10.

Similar orbit-surveys are carried out for the other dwarf members of the Galaxy group, and the results are given in Table 2; open circles and crosses given in the second and sixth columns represent respectively the existence and absence of the model-consistent orbits for the past 10.4 Gyr. Although these results are discussed later on the basis of

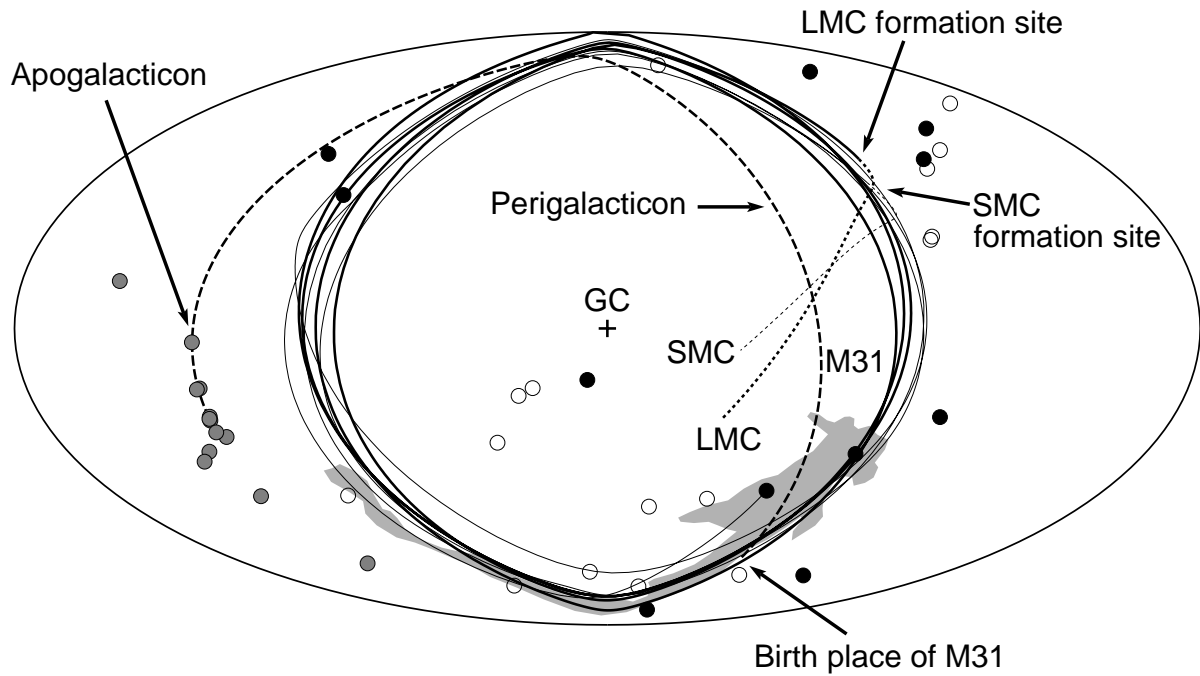


Fig. 8. Orbit of M31 and the LMC/SMC for the last 10.4 Gyr. Since they are projected onto the (l, b) -plane, this figure is topologically the same as figure 7. The formation site of the LMC/SMC is in the direction of $(l, b) = (278^\circ, 45^\circ)$. The extreme end of the dashed line is a birth place of M31, estimated in the flat universe of $H_0 = 75 \text{ km s}^{-1} \text{Mpc}^{-1}$.

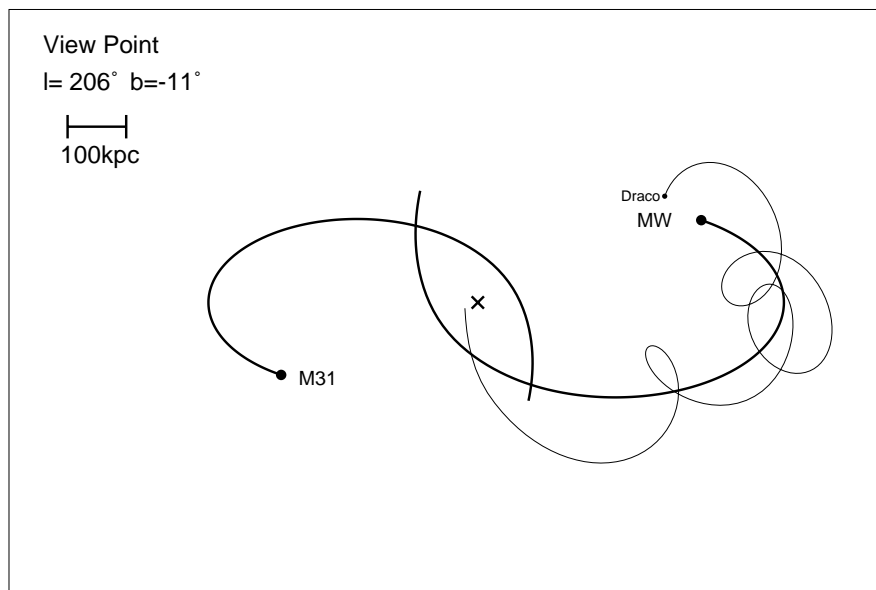


Fig. 9. Orbit of the dwarf spheroidal galaxy (Dsp) Draco projected onto the LGG plane. The formation site is the same as in figure 7.

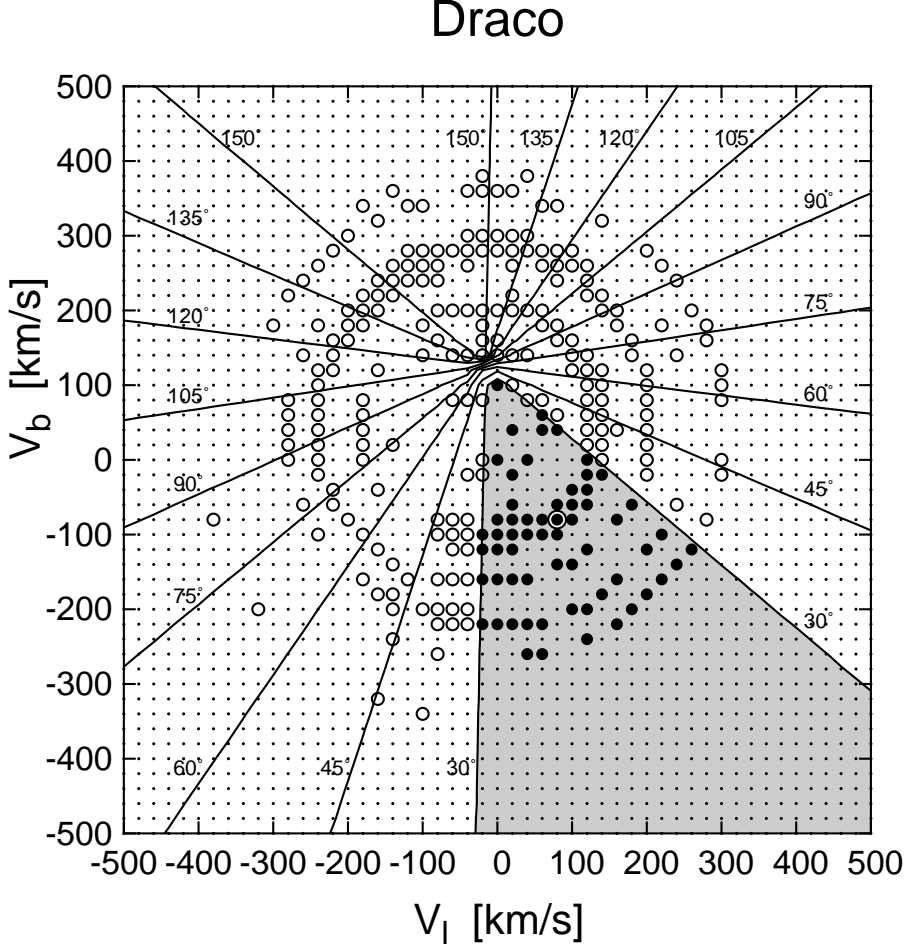


Fig. 10. Velocity diagram (V_l, V_b) of the tangential motion, prepared for tracing back-in-time the Draco's orbit until its birth place. If we choose velocities in the shaded region, the Draco's motion is confined within the LGG disk of finite thickness of 100 kpc, and moves in the same sense as driven hydrodynamically by the collision with M31. The orbit in figure 9 is obtained from the tangential velocity at the double circle.

more global model-picture, we can say here, at least, more than sixty percent of the Galaxy group members hold \bigcirc .

The Sagittarius dwarf galaxy, which was discovered by Ibata et al. (1994), is one of the four dwarfs not on the LGG ring (see figures 1 and 2) but near the direction of the Galactic center. It locates at only 16 kpc of the Galactic center and is elongated at a right angle against the Galactic plane. Such elongated structure of the Sagittarius is considered to represent a tidal disruption due to the Galaxy and its major axis should coincide approximately with the orbit round the Galaxy. Thus we can estimate the orbital plane of the Sagittarius by tracing its major axis and the Galactic center (Ibata et al. 1997). Using the estimated orbital plane together with the data in Table 1 and our model conditions for the LGG origin, we have computed the model orbit of the Sagittarius dwarf galaxy, and obtained the result of \bigcirc and the prediction for proper motion in the (l, b) directions in Table 2. It is qualitatively consistent with that given in Ibata

et al. (2001).

Next we searched for model-fitting orbits of the M31 group dwarfs in the same way as in cases of the Galaxy group. Two orbits of NGC185 and NGC205 thus obtained are presented in figure 11 over their lifetime of 10.4 Gyr. They are actually confined within the flat disk of finite thickness (figure 3), and fulfill our model conditions that they pass the formation site exactly 10.4 Gyr ago.

Fourteen dwarf galaxies out of thirty nine members (Table 1) belong neither to the Galaxy nor to M31, but are located just like linking these two massive galaxies (figure 3). One of them, Pegasus, has orbit that follows our model scenario. A particular interest may also be in examining whether or not our model orbits of NGC205 and M32 are consistent with those determined by Sato & Sawa (1986) and Byrd (1976) who claimed that the warp of hydrogen gas distribution at the outer parts of M31 and the peculiar motion of hydrogen gas near the center of M31 are due to the tidal interaction with NGC205 and

Table 2. A sheet of score for model orbits and their proper motions to be measured, if possible, at present. The LGG members whose orbits agree with our model scenario have a mark \bigcirc , and those that do not agree \times . The proper motion μ_l and μ_b of each galaxy with \bigcirc is given in $\mu\text{as yr}^{-1}$ in the last two columns.

Galaxy	score	μ_l	μ_b	Galaxy	score	μ_l	μ_b
WLM	\times	—	—	Leo A	\times	—	—
NGC55	\times	—	—	Sextans B	\times	—	—
IC10	\bigcirc	41	-61	NGC3109	\times	—	—
NGC147	\bigcirc	35	12	Antlia	\times	—	—
And III	—	—	—	Leo I	\bigcirc	-17	-152
NGC185	\bigcirc	41	20	Sextans A	\times	—	—
NGC205	\bigcirc	31	-88	Sextans	\bigcirc	-49	245
M32	\bigcirc	37	-115	Leo II	\bigcirc	21	-93
M31	\bigcirc	38	-49	GR8	\times	—	—
And I	—	—	—	Ursa Minor	\bigcirc	256	-128
SMC	\bigcirc	-730	1360	Draco	\bigcirc	206	-206
Sculptor	\bigcirc	-347	1090	Milky Way	\bigcirc	—	—
LGS3	\bigcirc	89	-130	Sagittarius	\bigcirc	-3520	1850
IC1613	\bigcirc	72	-36	SagDIG	\times	—	—
And II	—	—	—	NGC6822	\times	—	—
M33	\bigcirc	90	-80	DDO 210	\times	—	—
Phoenix	\bigcirc	-9	180	IC5152	\times	—	—
Fornax	\bigcirc	275	474	Tucana	—	—	—
EGB0427+63	\times	—	—	UKS2323-326	\times	—	—
LMC	\bigcirc	-420	1720	Pegasus	\bigcirc	-31	-57
Carina	\bigcirc	20	522				

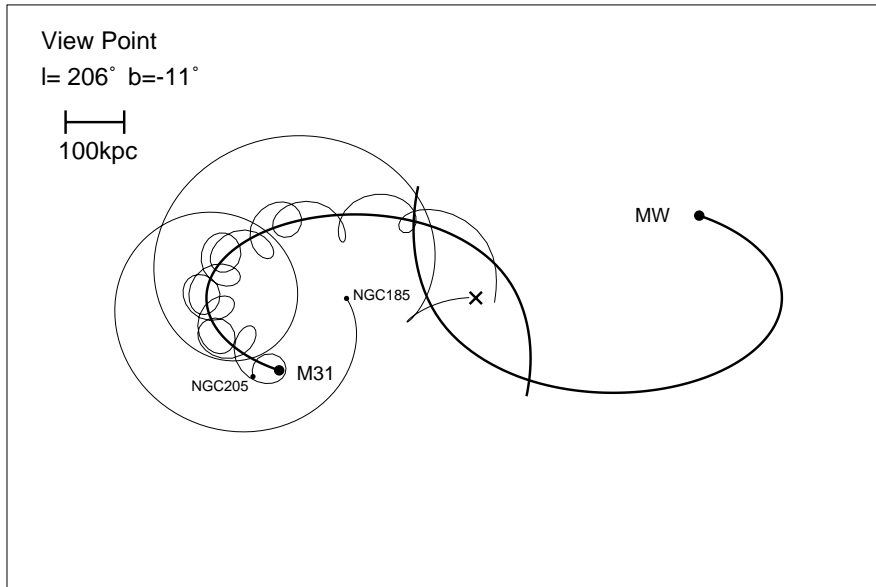


Fig. 11. Same as figure 9, but the orbits of NGC185 and NGC205 of the M31 group.

M32, respectively. According to Sato & Sawa (1986) the orbital plane of NGC205 makes a large angle of $\sim 90^\circ$ against the M31 disk and the direction of motion is counterclockwise seen from $(l, b) = (206^\circ, -11^\circ)$. These orbit features are consistent with in figure 11. Similarly, the orbital plane of M32 makes a medium angle against the M31

disk and the sense of revolution around M31 (Byrd 1976) are consistent with that inferred from the kinematics of our off-center collision between M31 and the Galaxy.

We mention that the model orbits for these two galaxies are determined easily, because NGC205 and M32 are so close to M31, 20 to 40 kpc from its center, and, therefore,

they are located already deep within the LGG disk of 50 to 100 kpc thickness. Since the scale of the formation site of $\sim 50 - 100$ kpc is much larger than the above mentioned 20 to 40 kpc, we can choose their suitable proper motion in considerably wide ranges of the (V_l, V_b) diagram as in figure 10.

Ibata et al. (2001) and Irwin et al. (2001) determined the orbit of M32 by use of the data of stellar streaming in M31. It is shown easily to be consistent with our model orbit. At present, however, we do not have enough data to conclude which is more agreeable to our model, Byrd's orbit (Byrd 1976) or Ibata's one (Ibata et al. 2001).

Again we give in Table 2 the results, \bigcirc and \times , for our orbit search for the members of the M31 group, together with the results for the nongroup members.

Finally we show in figures 12 and 13 all orbits of the members of the LGG with \bigcirc in Table 2: Figure 12 gives a face-on view seen from the direction of $(l, b) = (206^\circ, -11^\circ)$ while figure 13 an approximately edge-on view from the direction of $(296^\circ, -11^\circ)$. Although the orbits are much tangled each other and it is very hard to derive their detailed numerical data, we can see globally that the LGG dwarf galaxies are driven to form by the ancient off-center collision between M31 and the Galaxy, and that they evolve dynamically on the orbital plane of these two massive galaxies.

6. Angular Momentum and Dark Matter Problems in the LGG Model

We have made a hydrodynamical model for the origin of the orbital angular momentum of the Magellanic Cloud System, and also for the hydrodynamically-driven formation of the dwarf members of the LGG. If our model is realistic, the orbits of the LGG members and their formation sites can be determined theoretically. However, we still have some problems that should be discussed from the viewpoint of the present model.

6.1. Tidal torque on the primordial disks of the Galaxy and M31

At the close passage of M31 at ~ 150 kpc from the Galactic center (figure 5(a)), the tidal torque N works on the disk, which could spin it up in the same direction as that of the orbital angular momentum of the Magellanic Cloud System about the Galaxy. It is perpendicular to the present disk of the Galaxy. This dynamics should be exert the same effect on the disk of M31, too.

The gravitational torque is the monopole-quadrupole moment interaction. That is, $N \propto M/d^3$, where M is the mass of the nearby passing galaxy and d is the impact parameter or the distance of the perigalacticon. Note that N is not proportional to d^{-2} but to d^{-3} .

We can estimate how much a spin has been given to the Galactic disk through the off-center collision with M31. Here we use conveniently the dynamics of the warping of hydrogen gas disk of the Galaxy that was modeled theoretically by the close approach of the Magellanic Cloud System at ~ 15 kpc of the Galactic center (Fujimoto &

Sofue 1976; Fujimoto & Sofue 1977). The torque, N_{LMC} due to the LMC, is,

$$N_{\text{LMC}} \propto M_{\text{LMC}} / (15 \text{ kpc})^3. \quad (15)$$

In the same way, the torque due to M31, N_{M31} , is represented as,

$$N_{\text{M31}} \propto M_{\text{M31}} / (150 \text{ kpc})^3. \quad (16)$$

The ratio of N_{M31} to N_{LMC} is,

$$\begin{aligned} \frac{N_{\text{M31}}}{N_{\text{LMC}}} &= \left(\frac{M_{\text{M31}}}{M_{\text{LMC}}} \right) \left(\frac{15 \text{ kpc}}{150 \text{ kpc}} \right)^3 \\ &\sim \frac{4 \times 10^{12} M_{\odot}}{2 \times 10^{10} M_{\odot}} \left(\frac{1}{10} \right)^3 = 0.2. \end{aligned} \quad (17)$$

The angular momentum of the warp of hydrogen gas is known to be only a small fraction of that of the disk, and it is negligibly small for the inner disk of 8 kpc in radius. Thus the ratio in equation (17) indicates that the torque due to M31, N_{M31} , is smaller than N_{LMC} , or our off-center collision between M31 and the Galaxy is not large to spin up the disk so that it becomes parallel to the orbital plane of the Galaxy-M31 system. Even if we take into account the duration of these torques, the spin of the disk is still small, only comparable to that of the observed warping of the disk (Fujimoto & Sofue 1976; Fujimoto & Sofue 1977).

The ratio in equation (17) has been obtained for the disk whose radius was ~ 15 kpc at the time of the off-center collision. If such a radius of the early disk was ~ 75 kpc, the magnitude of the quadrupole moment becomes five times and, therefore, the ratio in equation (17) is roughly unity,

$$\frac{N_{\text{M31}}}{N_{\text{LMC}}} \sim 1. \quad (18)$$

The gain of the angular momenta was still small for the early large Galactic disk. Again it would be only comparable to that of the present-day warp of the hydrogen disk.

We can thus infer from these data that the orbital angular momentum of the Magellanic Cloud System and the spin of the Galactic disk are of the different origin. These arguments may reflect the fact that the Galactic disk and the M31 disk are observed not parallel on the plane of the sky but make an angle of about 60° against each other.

Peebles (1969) and Thuan & Gott III (1977) presented a tidal model that the gravitational torque due to the nearby passing M31 can spin up the disk of the Galaxy. However, the model parameter values and basic assumptions adopted there are very different from those used in this study: The epoch of the interaction between the Galaxy and M31 is 12-13 Gyr ago; the M31's orbit is straight, passing by the Galaxy and changing its direction in the neighborhood; the proto-Galaxy is already in an elongated flat disk with 100 kpc length directed towards M31.

6.2. Dark matter in dwarf members

Some of the LGG dwarfs have large amounts of dark matter, inferred from their high mass-to-light ratios of

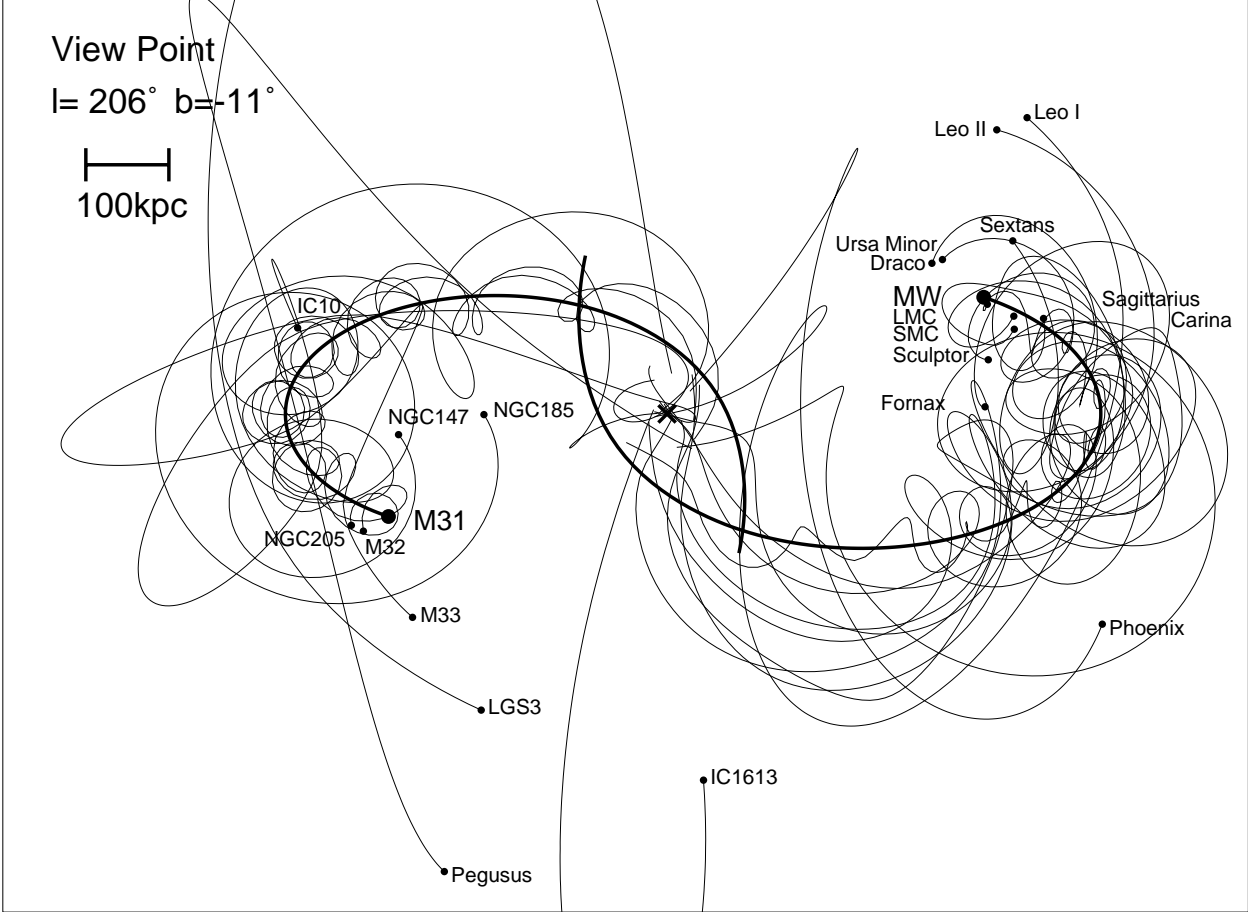


Fig. 12. Face-on view of orbits of the LGG members, projected of the orbital plane of M31 and the Galaxy. All dwarf members in this diagram start from their common formation site and arrive at their present positions as we see them today. The view is in the direction from $(l, b) = (206^\circ, -11^\circ)$.

Draco, Sextans and Ursa Minor (van den Bergh 2000), although it is still uncertain that many other dwarfs do not have dark matter. The present model for the LGG origin gives no answer to the question; why dark matter is not distributed equitably to all dwarf members of the LGG.

We present here a possible explanation by using figure 14 in which halo models of the proto-Galaxy and proto-Andromeda are given at the time just before encountering or grazing each other (figure 5(a)), with a relative velocity of $\sim 400 \text{ km s}^{-1}$.

The halo comprises baryonic matter clouds and dark matter clouds, some of which occupy the same space while others do not. The mean random velocity of the clouds is $\sim 220 \text{ km s}^{-1}$, resembling the unorganized motion in the gravitational potential of isothermal mass distribution.

From figures 14 and 5(a), we can suppose various types of collisions between these clouds. For example, the baryonic gas clouds 1 and 1' would collide to condense together

leading to the formation of a small mass galaxy, or dwarf galaxy with only a small amount of dark matter. Another example is a high velocity collision of dark matter clouds, 2 and 2', in the Galaxy halo and the M31 halo, respectively. They would penetrate each other without generating a dark matter clump. When the colliding velocity is small like between i and i' , or between a baryonic and dark matter clouds, the two-stream instability occurs to form a gravitating matter clump or a dwarf galaxy with a large amount of dark matter. The following dispersion relation given in Saslaw (1987) would be convenient for these analyses,

$$\lambda_{\text{crit}} = \frac{c^2 - u^2}{[\langle v_d^2 \rangle (\rho_g / \rho_d) + 2(c^2 - u^2)]^{1/2}} \lambda_{\text{Jd}}. \quad (19)$$

Here c is the sound velocity in the baryonic gas which has the density of ρ_g and streams with velocity of u relative to the dark matter whose density is ρ_d and velocity dispersion is $\langle v_d^2 \rangle$. The dark matter has a Jeans length

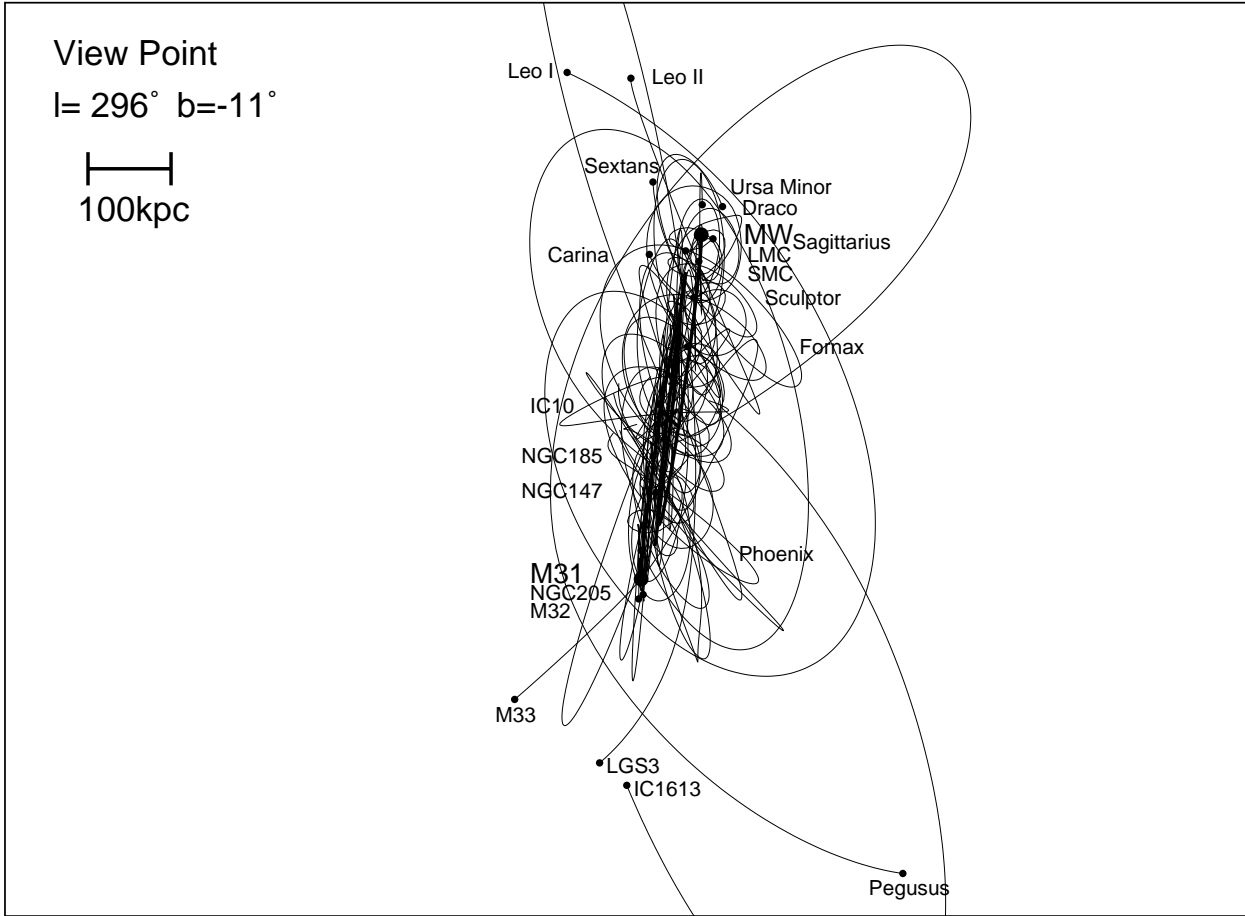


Fig. 13. Same as in figure 12, but an edge-on view. Most of orbits are contained in the LGG disk of finite thickness. The view is in the direction from $(l, b) = (296^\circ, -11^\circ)$.

given by λ_{Jd} . When u is large, the collision would disperse the baryonic and dark matter clumps, resulting in neither condensation nor formation of small mass galaxies.

We can assume other various collisions such as multiple ones, i , $i+1$ and i' . In other words, it is not so unrealistic that the dwarf member of the LGG is a mixture of baryonic and dark matters in various ratios. This dark matter model, shown schematically in figures 14 and 5(a), is, of course, *ad hoc* and far from conclusive, remaining very open to further investigations.

7. Discussion and Conclusion

On the bases of the ring-like distributions of the Local Group of Galaxies and the Magellanic Stream on the plane of sky (seen in the two-dimensional space), and of their coplanar distribution seen also in the three-dimensional space, we have proposed a dynamical model for the origin and evolution of the dwarf members of the LGG: The primordial dwarfs, the primordial LMC and SMC as well,

were driven to form in the high density region of gas generated hydrodynamically by the off-center collision between the primordial gas-rich M31 and the primordial gas-rich Galaxy some 10 Gyr ago. Newborn dwarf galaxies are scattered on the orbital plane of these two massive galaxies and they are trapped either to the potential well of the Galaxy or to that of M31, while other some number of dwarfs are left behind from such trappings. The latter objects are observed as if linking the Galaxy and M31 groups.

The orbital motion of M31 (relative to the Galaxy) is determined so that it successfully reproduces the well-studied dynamics and history of the LMC/SMC system. The most important model scenario is that the LMC/SMC are born from the high-density gas of the formation site, together with other dwarf members of the LGG simultaneously. Thus the orbital plane of M31 must be parallel to that of the LMC/SMC, roughly normal to the line joining the present position of the sun and the Galactic center. Both M31 and the LMC/SMC revolve

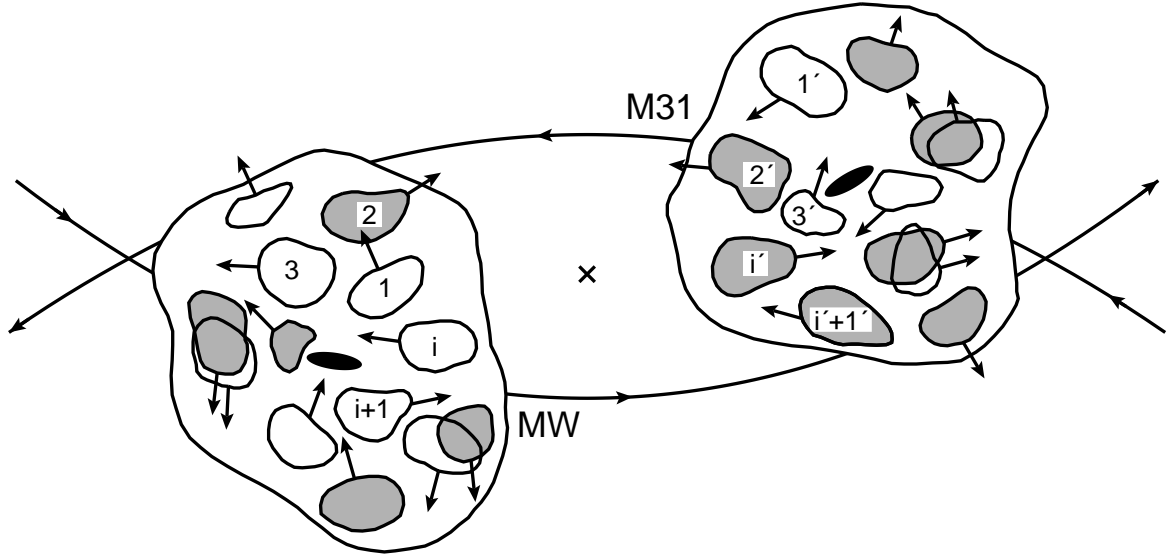


Fig. 14. Schematic view of model for primordial halos of the Galaxy and M31 at the time when they graze each other as in figure 5(a). Baryonic gas fluctuations and dark matter fluctuations are shown respectively by white and shaded contours, numbered with $1, 2, \dots, i, i+1, \dots$ in the Galaxy, and $1', 2', \dots, i', i'+1', \dots$ in M31. Some contours coincide spatially and others do not, modeling the fact that the gravitational force works similarly on the baryonic and dark matters, but other forces due to pressure, magnetic field and radiation work on the baryonic gas. The solid lines indicate the orbits of the Galaxy and M31 about their center of mass. The relative velocity is $\sim 400 \text{ km s}^{-1}$. Velocity arrows attached to the clouds mimic the mean random velocity of approximately 220 km s^{-1} in the proto-Galaxy halos and 250 km s^{-1} in the proto-M31 halos.

round the Galaxy counterclockwise seen from the sun, on the unclosed elliptical orbit.

Thus we could have an answer to a long-standing question what the origin of the LMC/SMC system is and where their large orbital angular momenta come from. Moreover interestingly, we could identify the birth places of M31 and the LMC/SMC on the sky and in the space, if precise age of the universe is given.

We are unable to demonstrate theoretically the validity of our dynamical model only from the data about the dwarf members: their positions on the sky (l, b), radial velocities and radial distances measured from the Galactic center. Therefore, instead, we have searched for the dwarf members' past orbits that follow the model scenario. Figures 12 and 13 can actually show that the dwarf members start from their common formation site, move on the orbital plane (figure 13), and arrive at the present positions, reproducing the ring-like distribution in figures 3 and 4.

From the results in Table 2 we find finally that more than sixty percent of the LGG members (22 out of 35) have \bigcirc , suggesting our dynamical model for the LGG is very realistic.

The dwarf members marked with \times in Table 2 do not have their orbits that can be traced back in time to the formation site in our model scenario. They could be objects that plunged into the spherical LGG region from outside, or their orbits have been bent gravitationally by other nearby massive galaxies. We could also consider

that these objects are intrinsic dwarfs born directly from the expanding universe and left behind from their merger to M31 and/or to the Galaxy, although we have again a question why such cosmologically early-formed objects tend to gather in the LGG disk.

On the other hand, if we relax our model conditions in such a way that the LGG dwarfs are formed due also to the tidal disturbance in gas around M31 and the Galaxy, then the formation site depicted in figure 5(a) would be largely extended on their orbital plane. See a recent HST picture and its caption for dwarf formation in the Stephan's Quintet (Weaver et al. 2001). The number of \bigcirc in Table 2 will increase, although it becomes difficult to predict the dwarfs' proper motions.

A small mass spiral, M33, has been treated as a test-particle in determining the orbits of the LGG members. It is, of course, not correct in a sense that the mass of M33 is three to four times as large as that of the LMC/SMC system. It is necessary to join this spiral to our four-body problem, but we do not yet have a key phenomenon and/or theory how to include M33 in a new five-body dynamics of the Galaxy-M31-M33-LMC-SMC in the LGG region. A fragmentary chain of hydrogen gas is observed as if bridging M33 and M31 (Blitz et al. 1999), and this may be usable to determine the M33 orbit. However, we remain open to a conclusion if it is in the same category as the Magellanic Stream. Even if the gravity of M33 is taken into account, however, we believe that our conclusions do not change so significantly, because the total mass of the

Galaxy and M31 dominates that of all other members and control them gravitationally.

We did not use the data about the tidal-cut-off radii of the LGG dwarfs, because, as figures 12 and 13 show, they could be located close to the Galaxy, or M31 or to both before they become condensed to dwarf galaxies. Even if the pericenter distance of a dwarf's orbit is calculated formally from the tidal-cut-off-radii data, we cannot know what it means in our LGG model.

Yoon & Lee (2002) found a group of metal-poor star-clusters (counted as seven at the moment) and showed that these clusters align on the plane perpendicular to the line joining the present position of the sun and the Galactic center, in quite a similar way to that discussed about the LGG members in figures 1 and 2. As they suggest, if these metal-poor clusters were born originally in the LMC and have been captured recently to the Galaxy, some of the globular clusters in the Galactic halo are regarded as tightly related to the LGG dynamics that the LMC was driven to form at the off-center collision between M31 and the Galaxy.

We have pursued backward in time M31 and the LMC/SMC in an expanding flat universe. When the present model proves to be realistic and is improved to be more quantitative, we must reexamine various parameters applied so far. For example, a claim may be made that the lifetime of 10.4 Gyr for the LGG model is a little too small and ~ 12 Gyr more suitable. The former age has been obtained by use of the masses of the Galaxy and M31 which are applied uniformly in their series of papers by Murai & Fujimoto (1980), Gardiner et al. (1994), Fujimoto et al. (1999) and Sawa et al. (1999). However, if we take a-little-less masses for the Galaxy (Prada et al. 2003) and M31, or their smaller radii of dark matter halos, it is possible that the latter age is more reasonable. At present, however, we must wait for a moment to conclude which is more realistic and more contribute to understanding the origin and evolution of the LGG.

We have only briefly touched upon some problems such as the tidal effect on the disks of the Galaxy and M31, the dark matter mass-fraction among the LGG dwarfs, and etc. The extensive studies on these problems would contribute to obtaining new hints to improve and develop more realistically our LGG model.

We would like to thank Professor Y. Kumai for his critical comments and discussions about the present work, and one of us (M.F) deeply thanks Vice-President of Nagoya University K. Yamashita for his hospitality and research support during my stay at his U-Lab., Department of Physics and Astrophysics.

References

Binney, J & Tremaine, S. 1987, Galactic Dynamics (Princeton University Press)

Blitz, L., Spergel, D. N., Teuben, P. J., Hartmann, D., & Burton, W. B. 1999, ApJ, 514, 818

Byrd, G. G. 1976, ApJ, 208, 688

Byrd, G., Valtonen, M., McCall, M., & Innanen, K. 1994, AJ, 107, 2055

Deeg, H. J., Munoz-Tunon, C., Tenorio-Tagle, G., Telles, E., Vilchez, J. M., Rodriguez-Espinosa, J. M., Duc, P. A., & Mirabel, I. F. 1998, A & AS, 129, 455

Einasto, J., Saar, E., Kaasik, A., & Chernin, A. D. 1974, Nature 252, 111

Fich & Tremaine 1994, ARA&A, 29, 409

Fujimoto, M., Sawa, T., & Kumai, Y. 1999, IAU Symp., 186, 31

Fujimoto, M. & Sofue, Y. 1976, A & A, 47, 263

Fujimoto, M. & Sofue, Y. 1977, A & A, 61, 199

Gardiner, L. T., Sawa, T., & Fujimoto, M. 1994, MNRAS, 266, 567

Gardiner, L. T., & Noguchi, M. 1996, MNRAS, 278, 191

Gott III, J. R., & Thuan, T. X. 1978, ApJ, 223, 426

Hartwick, F. D. A. 2000, AJ, 119, 2248

Hodge, P. 1992, The Andromeda Galaxy (Kluwer Academic Press, Dordrecht)

Ibata, R. A., Gilmore, G., & Irwin, M. J. 1994, Nature, 370, 194

Ibata, R. A., Lewis, G. F., Irwin, M. J., Totten, E., & Quinn, T. 2001, ApJ, 551, 294

Ibata, R. A., Wyse, R. F. G., Gilmore, G., Irwin, M. J., & Suntzeff, N. B. 1997, AJ, 113, 634

Irwin, M., Ferguson, A., Tanvir, N., Ibata, R. A., & Lewis, G. 2001, Science, 5, 3, October

Kahn, F. D., & Woltjer, L. 1959, ApJ, 130, 705

Kunkel, W. E. 1979, ApJ, 228, 718

Landau, L. D. & Lifshit, E. M. 1975, The Classical Theory of Fields (Pergamon, New York)

Lin, D. N. C., & Lynden-Bell, D. 1982, MNRAS, 198, 707

Lynden-Bell, D. 1999, IAU Symp. 192, 39

Majewski, S. R. 1994, ApJ, 431, L17

Mateo, M. L. 1998, ARA&A, 36, 435

Mathewson, D. S., Cleary, M. N., & Murray, J. D. 1974, ApJ, 190, 291

Mishra, R. 1985, MNRAS, 212, 163

Murai, T., & Fujimoto, M. 1980, PASJ, 32, 581

Peebles, P. T. E. 1969, ApJ, 155, 393

Peebles, P. J. E. 1993, Principles of Physical Cosmology (Princeton University Press, Princeton)

Prada, F., Vitvitska, M., Klypin, A., Holtzman, J. A., Schlegel, D., Grebel, E., Rix, H.-W., Brinkmann, J., McKay, T. A., & Csabai, I. 2003, ApJ, 598, 260

Raychaudhury, S., & Lynden-Bell, D. 1989, MNRAS, 240, 195

Saslaw, W. C. 1985, *Gravitational Physics of Stellar and Galactic System*, Cambridge University Press. London New York.

Sato, N. R., & Sawa, T. 1986, PASJ, 38, 63

Sawa, T., Fujimoto, M., & Kumai, Y. 1999, IAU Symp., 190, 499

Thuan, T. X. & Gott, J. R. III 1977, ApJ, 216, 194

Tully, R. B. 1988, *Nearby Galaxies Catalog* (Cambridge University Press, Cambridge)

van den Bergh, S. 2000, *The Galaxies of the Local Group* (Cambridge University Press, Cambridge)

Wannier, P., & Wrixon, G. T. 1972, ApJ, 173, L119

Weaver, D., Gallagher, S., Charlton, J., & Kennedy, B. 2001, STSCI-PR01-22, *Hubble Space Telescope News*

Westerlund, B. E. 1997, *The Magellanic Clouds* (Cambridge University Press, Cambridge)

Yoon, S. J., & Lee, Y. W. 2002, Science 297, 578